JOURNAL OF EXPERIMENTAL AND THEORETICAL PHYSICS, 2024, Vol. 166, No. 1(7), pp. 121–136

MAGNETIC FIELDS IN THE NEAR-LUNAR PLASMA: PROPERTIES, MANIFESTATIONS, EFFECTS

© 2024 L. M. Zelenyi*, S. I. Popel, A. P. Golub**

Space Research Institute of the Russian Academy of Sciences 117997, Moscow, Russia

**e-mail: lzelenyi@cosmos.ru*

***e-mail: popel@iki.rssi.ru*

Received February 27, 2024

Revised March 15, 2024

Accepted March 15, 2024

Abstract. Possible manifestations of magnetic fields in the near-lunar plasma are considered. It is noted that due to the action of magnetic fields in the Earth's magnetotail, the transport of charged dust particles over large distances above the lunar surface is possible. Accordingly, dusty plasma above the sunlit lunar surface can exist for the entire range of lunar latitudes. Due to significant localization of magnetic anomaly regions, their influence on the transport of charged dust particles over the Moon is insignificant. Nevertheless, it is shown that in magnetic anomaly zones, dusty plasma is "suppressed" compared to the situation outside these zones dusty plasma. Important objects of study are mini-magnetospheres associated with lunar magnetic anomaly zones and responsible for a number of optical and satellite observations, such as "lunar swirls," lower-hybrid turbulence, etc.

Article for the special issue of JETP dedicated to the 130th anniversary of P. L. Kapitsa

DOI: 10.31857/S004445102407e137

1. INTRODUCTION

In the life of Pyotr Leonidovich Kapitsa, there was a relatively short period that began in 1946 when, due to a conflict with L.P. Beria, he fell into serious disgrace and was removed from the position of director of the Institute for Physical Problems of the USSR Academy of Sciences, which he had founded in 1934. P. L. Kapitsa remained in disgrace for nine years. During this time, he mainly lived at his dacha in Nikolina Gora. But he did not stop doing physics: he became interested in a new field – high-power electronics and plasma physics. At the dacha, he again founded IFP, only this time it was not the Institute for Physical Problems, but the "Physics Problems Hut" – as Kapitsa called his home laboratory, where he created his first high-frequency high-power generators.

Thus, it can be said that plasma physics is also part of the extensive range of Kapitsa's scientific interests and accomplishments. Moreover, Pyotr Leonidovich witnessed the exciting competition for primacy in lunar exploration between the USSR and USA in the 1960s-1970s, and the plasma physics of the lunar exosphere, whose importance was just beginning to be realized in those years, would certainly have interested him. Given P. L. Kapitsa's great interest in magnetic field physics, this work presents material dedicated to the influence of magnetic fields on the lunar exosphere plasma.

One of the key problems in near-lunar space physics currently is the study of interactions between near-lunar plasma and magnetic fields. Although magnetic fields near the Moon are rather small, they can lead to interesting and quite noticeable consequences. Near-lunar plasma is subject to two types of magnetic fields. First of all, this is the Earth's magnetosphere tail field, whose typical values are on the order of $10^{-5} - 10^{-4}$ Gs [1, 2]. The Moon is located in the Earth's magnetosphere tail for about a quarter of its orbit. Additionally, there are so-called magnetic anomaly regions on the Moon, associated with magnetic material in the lunar crust. Measurements of near-surface magnetic fields on

the visible side of the Moon, performed during Apollo missions and 16, were respectively $3.8 \cdot 10^{-4}$, $1.03 \cdot 10^{-3}$, $3 \cdot 10^{-5}$ and $3.27 \cdot 10^{-3}$ Gs [3]. Satellite measurements have shown [4] that the strongest (for the Moon) magnetic fields are present on the far side of the Moon. These fields are believed to determine the limb disturbances of the solar wind.

The question of the origin of magnetic fields in magnetic anomaly zones remains open. Accordingly, theoretical studies of magnetic fields on the Moon are mainly devoted to identifying the causes of magnetic fields on the Moon (see, for example, [5–7]). One hypothesis about the origin of magnetic fields suggests that the Moon once had a magnetic dynamo driven by thermal processes. However, due to, in particular, the small size of the lunar core, this theory proves problematic [8]. Another hypothesis is that impact events could either create or enhance pre-existing magnetic fields, especially near the antipodes of the largest craters [9]. However, this hypothesis also has contradictions with observational results, as well as with the fact that powerful impact events necessary for generating magnetic fields within this hypothesis could either bring the Moon out of synchronous rotation or cause large-amplitude librations that would last for several tens of thousands of years [10]. There is a hypothesis suggesting an alternative mechanism for creating a lunar dynamo, in which the energy for dynamo action comes from the Moon's rotation rather than from thermal effects [5].

When describing the interaction of near-lunar plasma with magnetic fields, it is important to first consider the fact that plasma in the lunar vicinity should often be considered as dusty [11, 12]. Lunar regolith particles [13] are considered as the dust component above the Moon's surface, lifted either by electrostatic processes (see, for example, [14–20]) or due to meteoroid impacts [21–23]. Both types of dust particles contribute to the Moon's "dusty" exosphere. The most "powerful" plasma-dust exosphere is concentrated above the Sun-facing side of the Moon, which is under the influence of solar wind and radiation. In this environment, the photoelectric effect plays an important role, through which the Moon's surface illuminated by sunlight acquires a positive charge [24]. As a result, the dusty plasma above the illuminated side of the Moon contains solar wind electrons and ions, levitating dust particles, and photoelectrons entering the exosphere due to photoemission from the lunar surface and from the surfaces of levitating dust particles. In 2013, the United States carried out the NASA LADEE (Lunar Atmosphere and Dust Environment Explorer) mission [25], which studied near-lunar dusty plasma through orbital observations. Near the Moon's surface, dust was studied as part of the People's Republic of China's Chang E-3 mission [26]. In Russia, lunar missions Luna-26 and Luna-27 are being prepared (see, for example, [12, 27, 28]), which include studies of dust and dusty plasma properties in lunar orbit and near the lunar surface. The International Lunar Research Station project, involving Chinese and Russian scientists among others, also includes lunar dust research.

Solar wind, interacting with magnetic anomalies on the Moon's surface, leads to the formation of so-called mini-magnetospheres [29–33]. The analysis of mini-magnetospheres is of great interest for fundamental plasma physics. Their appearance in the lunar exosphere means that external (satellite) measurements are possible, including particle distribution functions. The fact that they are located on the closest planetary body to us also provides a high level of observational diversity. Of particular interest is also the connection between mini-magnetospheres and "lunar swirls" [34]. Swirls are exposed silicate materials whose albedo has been selectively preserved over time due to space weathering through the deflection of solar wind ion bombardment [35].

This paper examines possible manifestations of magnetic fields in near-lunar plasma. The article is partially a review. It describes some previously studied effects while presenting several new results, mainly concerning the influence of magnetic fields in magnetic anomaly regions on the formation of dusty plasma above the Moon. The description of the Earth's magnetotail magnetic fields' influence is provided in Section 2. Section 3 discusses the influence of magnetic fields in the regions of lunar magnetic anomalies. Section 4 briefly summarizes the results.

2. INFLUENCE OF MAGNETIC FIELDS IN THE EARTH'S MAGNETOSPHERE TAIL

The Moon moves in orbit at a speed of about 1 km/s [18]. Thus, considering that the dusty plasma near the Moon is "bound" to its surface, there is a

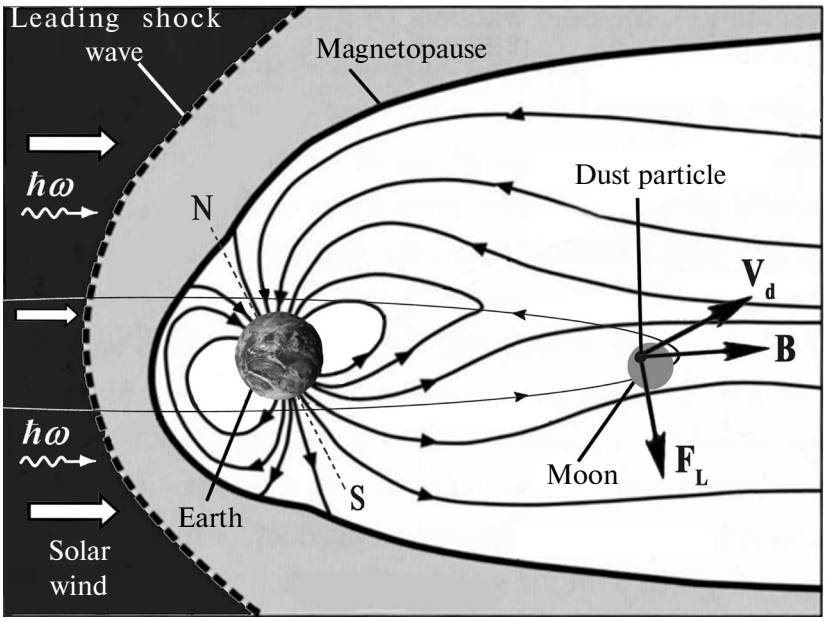

Fig. 1. Schematic representation of the Moon's movement in the Earth's magnetotail. The lunar orbit is shown by a thin line, arrows on the lunar orbit indicate the Moon's direction of motion. Solar wind and solar radiation photons are also shown ($\hbar\omega$).

relative velocity of charged dust particles with respect to the magnetic field lines of Earth's magnetosphere, having an order of 1 km/s. Consequently, despite even small values of magnetic field induction near the Moon, the appearance of a quite noticeable (due to large values of relative velocity) magnetic component of the Lorentz force acting on a dust particle is possible. Schematically, the Moon's movement in the Earth's magnetosphere tail, the magnetic field induction vector $\mathbf{B}$, dust particle velocity $\mathbf{v}_d$, and the magnetic component of the Lorentz force $\mathbf{F}_L$ are shown in Fig. 1.

Below, we consider manifestations [36] caused by the action of the magnetic component of the Lorentz force in the Earth's magnetosphere tail on the movement of charged dust particles in the Moon's "dusty" exosphere, as well as the possibility of generating lower hybrid waves in the near-lunar dusty plasma [20].

2.1. Equations for Describing Dust Dynamics

The dynamics of a charged dust particle above the lunar surface is determined by the equation describing Newton's second law, which takes into account the electrostatic and magnetic parts of the Lorentz force, as well as gravity:

$$m_d \frac{d^2\mathbf{r}_d}{dt^2} = q_d\mathbf{E} + \frac{q_d}{c}\mathbf{v}_d \times \mathbf{B} + m_d\mathbf{g}_0. \qquad (1)$$

Here m_d is the mass of the dust particle, $\mathbf{r}_d$ is its radius vector, $\mathbf{E}$ is the electric field, q_d is the charge of the dust particle, c is the speed of light, $\mathbf{g}_0$ is the acceleration of gravity near the lunar surface. The plasma surrounding the dust particle affects the parameters contained in the right-hand side of equation (1), and primarily the charge of the dust particle. The equation describing its charging has the form

$$\frac{dq_d}{dt} = I_e(q_d) + I_i(q_d) - I_{ph}(q_d) + I_{e,ph}(q_d), \qquad (2)$$

where $I_e(q_d)$ and $I_i(q_d)$ are microscopic currents of electrons and solar wind ions to the dust particle, $I_{ph}(q_d)$ is the photoelectric current of electrons from the dust particle due to the interaction of its surface with solar radiation, $I_{e,ph}(q_d)$ is the current of photoelectrons surrounding the dust particle to it. Expressions for these currents have the form

$$I_e \approx -\pi a^2 e n_{eS}\sqrt{\frac{8T_{eS}}{\pi m_e}}\left(1+\frac{Z_d e^2}{aT_{eS}}\right), \qquad (3)$$

$$I_i \approx \pi a^2 e n_{iS}\sqrt{\frac{T_{iS}}{2\pi m_i}}\frac{u_{Ti}}{u_i}\times$$

$$\times\left\{\frac{u_i+u_0}{u_{Ti}}\exp\left(-\frac{(u_i-u_0)^2}{2u_{Ti}^2}\right)+\right.$$

$$+\frac{u_i-u_0}{u_{Ti}}\exp\left(-\frac{(u_i+u_0)^2}{2u_{Ti}^2}\right)\Bigg\}+$$

$$+\pi a^2 e n_{iS}\sqrt{\frac{T_{iS}}{4m_i}}\frac{u_{Ti}}{u_i}\left\{\mathrm{erf}\left(\frac{u_i+u_0}{\sqrt{2}u_{Ti}}\right)+\right.$$

$$\left.+\mathrm{erf}\left(\frac{u_i-u_0}{\sqrt{2}u_{Ti}}\right)\right\}\left(1+\frac{2Z_d e^2}{aT_{iS}}+\frac{u_i^2}{u_{Ti}^2}\right), \quad (4)$$

$$I_{ph}\approx -\pi a^2 e N_0\sqrt{\frac{T_{e,ph}}{2\pi m_e}}\times$$

$$\times\left(1+\frac{Z_d e^2}{aT_{e,ph}}\right)\exp\left(-\frac{Z_d e^2}{aT_{e,ph}}\right), \quad (5)$$

$$I_{e,ph}\approx -\pi a^2 e n_{e,ph}\sqrt{\frac{8T_{e,ph}}{\pi m_e}}\left(1+\frac{Z_d e^2}{aT_{e,ph}}\right). \quad (6)$$

Here a is the size of the dust particle, Z_d — its charge number ($q_d = Z_d e$), e — elementary charge, $n_{e(i)S}$ is the concentration of solar wind electrons (ions), $T_{e(i)S}$ is the temperature of solar wind electrons (ions), $m_{e(i)}$ — mass of electron (ion), $u_0 = \sqrt{2Z_d e^2 / am_i}$, $u_{Ti} = \sqrt{T_{iS} / m_i}$ — thermal velocity of solar wind ions, u_i — is the solar wind velocity, $T_{e,ph}$ is the temperature of photoelectrons, N_0 is the concentration of photoelectrons at the lunar surface at the equator, $n_{e,ph}$ — concentration of photoelectrons depending on the height above the lunar surface for a given lunar latitude. Expressions (3)–(6) are valid for the case of positive charges of dust particles. Expression (5) for the current I_{ph} does not contain a factor containing radiation spectrum characteristics, which becomes possible in a situation where the surfaces of dust particles and the lunar surface have the same photoelectron work function W. In this situation, the specified factor can be expressed through the value N_0. The above system of equations is valid in the situation of rarefied near-surface dusty plasma near the Moon, when the influence of neighboring dust particles on each other can be neglected, which corresponds to the conditions existing on the Moon [12, 14].

When solving equations (1), (2), it is necessary to consider the following expression for the vertical component of the electric field E, formed by the charged surface of the Moon, depending on the height h above its surface:

$$E(h,\theta)=\frac{2T_{e,ph}}{e}\frac{\sqrt{\cos\theta/2}}{\lambda_D+h\sqrt{\cos\theta/2}}, \quad (7)$$

where λ_D is the Debye radius of photoelectrons at the Moon's surface, θ is the angle between the local normal and the direction to the Sun. Note that the angle θ for a smooth lunar surface (without hills and depressions) is approximately equal to the lunar latitude. This is due to the fact that the angle formed by the Moon's axis and the ecliptic plane is only 1.5424°.

Expression (7) is obtained as a result of jointly solving the kinetic equation for photoelectrons and the Poisson equation. The dependence of the electric field on the angle θ in expression (7) is due to the change in the number of photons absorbed per unit area of the Moon's surface, depending on the angle θ. The electric field distribution, similar to (7), was obtained in works [37–39].

For plasma parameters near the lunar surface, the term $q_d\mathbf{E}$ in the right-hand side of equation (1) exceeds the second term $(q_d / c)\mathbf{v}_d \times \mathbf{B}$ by at least five orders of magnitude. At first glance, this fact indicates the validity of approaches where the plasma-dust system above the Moon is studied without considering magnetic fields. However, such consideration, assuming a smooth (flat in a certain studied vicinity) lunar surface and taking into account only electrostatic and gravitational forces acting on a dust particle, can explain the lifting of dust particles only in a very limited range of angles θ ($|\theta| > \theta_0$), where θ_0 is determined from relation [39]

$$\sqrt{\cos\theta_0}\left|\ln(4\cos\theta_0)\right| = \frac{8\sqrt{2}\pi^2 a^2\rho^2 G R_M\lambda_D}{9}\left(\frac{e}{T_{e,ph}}\right)^2, \quad (8)$$

where ρ is the lunar regolith density, G is the universal gravitational constant, R_M is the Moon's radius. If we limit ourselves to considering dust particles with sizes not exceeding 1 μm (i.e., particles characteristic of the near-surface layer above the sunlit lunar surface [12, 14]), then we get that θ_0 does not exceed 76.14°. The reason for the above limitation is as follows. The motion of dust particles is determined by the competition between oppositely

directed electrostatic and gravitational forces. A dust particle uplift is possible only when the electrostatic force exceeds the gravitational force at the lunar surface. The electrostatic force is determined by the dust particle charge q_d, which is significantly influenced by the photoelectron concentration. In turn, the photoelectron concentration decreases with increasing $|\theta|$. At values of $|\theta|$, less than critical, the high concentration of photoelectrons surrounding the dust particle prevents it from acquiring a large positive charge sufficient for the electrostatic force to predominate over gravity. As a result, the dust particle cannot rise above the lunar surface. Thus, within the framework of a model that considers only electrostatic and gravitational forces acting on a dust particle, and assumes a smooth lunar surface (i.e., not accounting for the real surface profile), the emergence of dusty plasma is possible only in the range of angles $|\theta| > \theta_0$.

2.2. Calculation Results Considering the Magnetic Field of the Magnetosphere Tail

Taking into account the magnetic field of Earth's magnetosphere tail fundamentally changes the situation. As previously noted, approximately a quarter of the lunar orbit passes through Earth's magnetosphere tail. If we disregard the axis tilt and orbital inclination to the ecliptic plane for both Earth and Moon, then for approximately one-eighth of the lunar orbit, the magnetic component of the Lorentz force acting on a positively charged dust particle has a component directed along the Moon's surface towards its South pole (the situation shown in Fig. 1 and discussed below). After this, the magnetic field and the magnetic component of the Lorentz force reverse their direction. The movement of a positively charged dust particle occurs above the sunlit part of the Moon, and its exit from the region is possible $\theta > \theta_0$. If a positively charged dust particle, after entering Earth's magnetosphere tail, reaches the Moon's South pole (during the time the Moon covers one-eighth of its orbit) and consequently moves to the unlit side of the Moon, it will fall. If not, then after the Moon passes one-eighth of its orbit, the magnetic component of the Lorentz force will act in the opposite (northern) direction, and the dust particle (after its inertial movement for some time) will also change its direction of movement.

In calculations, we assume that there is a balance between electrostatic and gravitational forces in equation (1), i.e., the particle levitates at a certain height. The basis for this assumption is the adequate accounting for anomalous dissipation associated with the charging effect of dust particles in dusty plasma (see [40]). Anomalous dissipation suppresses deviations of dust particles during their motion from equilibrium trajectories, where the equality of absolute values of electrostatic and gravitational forces is approximately maintained. Further, in calculations, we neglect the axis tilt and orbital inclination to the ecliptic plane for both Earth and Moon. Then, defining $t = 0$ as the moment corresponding to the Moon's entry into Earth's magnetotail, we consider the magnetic field induction vector in the Moon's vicinity directed from north to south at $0 < t < 82$ h and from south to north at $82 < t < 164$ h. Fig. 2 shows the values characterizing the motion of dust particles of various sizes levitating above the lunar surface under the influence of Earth's magnetic field, for different moments of dust particle detachment from the lunar surface (and, accordingly, the beginning of levitation), $n_{eS} = n_{iS} = 8.7$ cm^{-3}, $T_{eS} = 12$ eV, $T_{iS} = 6$ eV, $u_i = 468$ km/s, $|\mathbf{B}| = 10^{-4}$ Gs, $W = 6$ eV, $T_{e,ph} = 1.9$ eV, $N_0 = 2.9 \cdot 10^2$ cm^{-3}. These values $T_{e,ph}$ and N_0 (see [12]) correspond to the solar maximum and quantum yield of lunar regolith given in [41].

Fig. 2 shows that due to the magnetic fields in Earth's magnetospheric tail, charged dust particles can be transported over large distances above the lunar surface, and consequently, dusty plasma above the sunlit lunar surface can exist for the entire range of lunar latitudes (from $-90°$ to $90°$). The transport of dust particles from lunar latitudes adjacent to the lunar poles ($|\theta| > 76°$), to the lunar equator due to the uncompensated magnetic component of the Lorentz force is a new qualitative effect that does not exist in the absence of a magnetic field. Note that the transport of dust particles is accompanied by changes in their charges. This fact is reflected in Fig. 3, which shows the time dependencies of the charge number Z_d for dust particles with a radius of 0.1 μm in situations corresponding to different moments of dust particle detachment from the lunar surface. The change in dust particle charge is related, in particular, to the fact that the number of photoelectrons surrounding the dust particle and affecting its charge depends on the angle θ. Additionally, the particle's charge is influenced

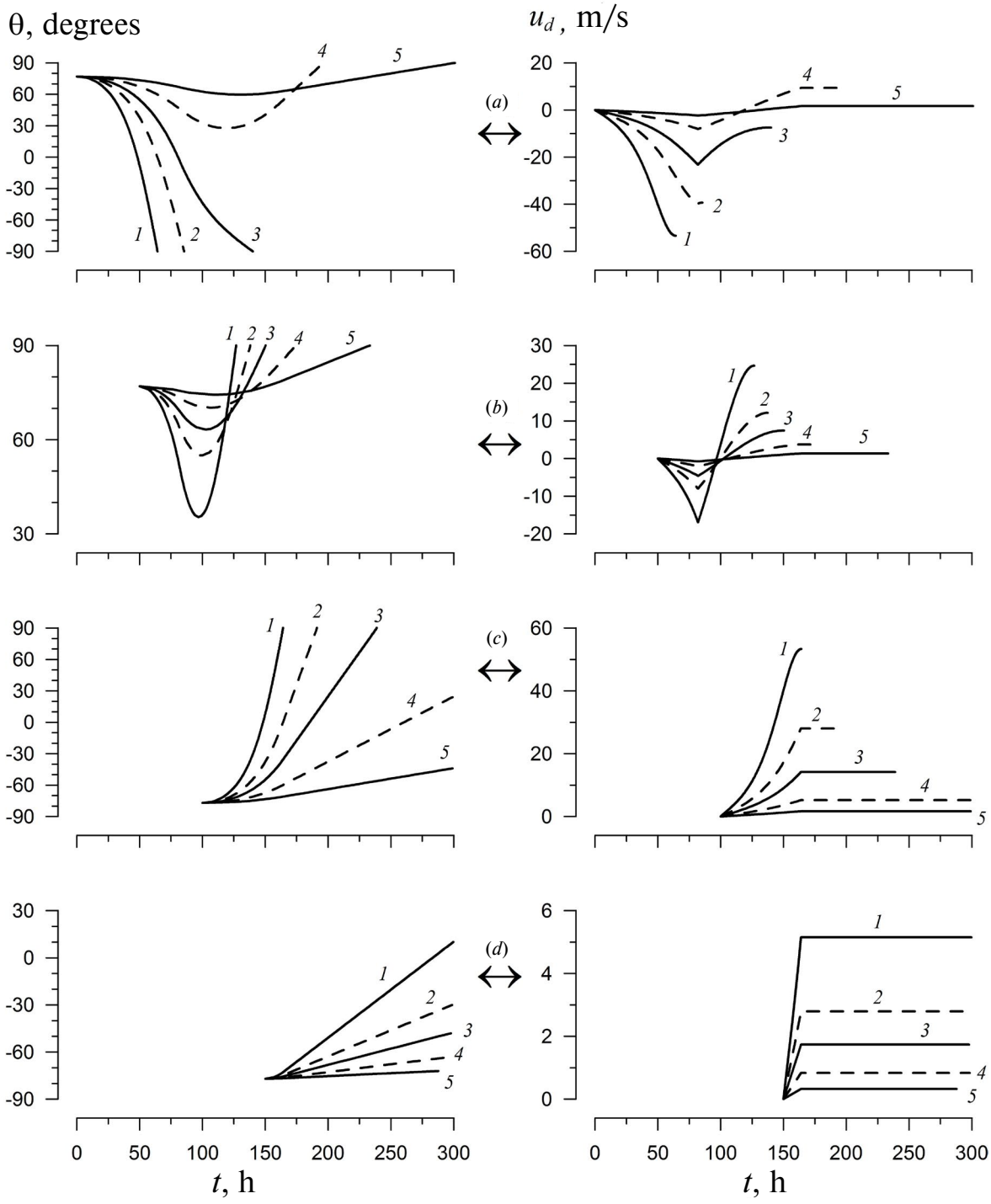

Fig. 2. Time dependencies of t angular coordinate θ and velocity component u_d of a dust particle along the lunar surface. The time moment $t = 0$ corresponds to the Moon's entry into the Earth's magnetotail. Curves *1–5* characterize dust particles with radii equal to 0.03 (*1*), 0.04 (*2*), 0.05 (*3*), 0.07 (*4*), 0.1 (*5*) μm. Results are shown for different moments of dust particles detachment from the lunar surface: 0 (*a*), 50 (*b*), 100 (*c*), 150 (*d*) h

by the height at which the dust particle is located. During transport, the height changes.

Thus, accounting for the influence of Earth's magnetospheric tail magnetic fields on dust transport above the lunar surface demonstrates the possibility of positively charged dust particles existing above the illuminated part of the Moon not only for angle values θ, exceeding 76.14°, but also for the entire

range of lunar latitudes (from -90° to 90°). Note that the consideration presented here does not take into account the influence of the lunar surface profile, which may provide additional arguments supporting the possibility of dusty plasma existence above the entire lunar surface.

2.3. Lower Hybrid Turbulence

The Moon's motion, along with the near-lunar plasma, relative to the magnetospheric tail plasma occurs at a speed of about 1 km/s. Moreover, during geomagnetic storms and substorms, particles with energies of about 10 keV trapped in radiation belts can penetrate into the magnetospheric tail [13, 42] and thus form charged particle flows in the magnetospheric tail. All this indicates the possibility of plasma instabilities developing in the regions of interaction between the lunar surface and the magnetospheric tail plasma, and thus speaks to the importance of wave processes in these regions. It turns out that lower hybrid turbulence is particularly important in this case, which can be excited throughout the interaction region of near-lunar dusty plasma and magnetospheric tail plasma [20].

The simplest instability leading to the generation of lower hybrid waves is a hydrodynamic instability of the Buneman type [43], described by the following linear dispersion equation (in the reference frame associated with the magnetospheric plasma):

$$1+\frac{\omega_{peM}^2+\omega_{pe(ph)}^2}{\omega_{Be}^2}\sin^2\Theta - \frac{\omega_{piM}^2+\omega_{peM}^2\cos^2\Theta}{\omega^2} - \frac{\omega_{pd}^2}{(\omega-\mathbf{k}\cdot\mathbf{u})^2}-\frac{\omega_{pe(ph)}^2\cos^2\Theta}{(\omega-k_\parallel u_\parallel)^2}=0. \quad (9)$$

Here k is the wave vector, ω is the frequency, ω_{peM} — plasma frequency of magnetospheric electrons, $\omega_{pe(ph)}$ — plasma frequency of photoelectrons, ω_{pd} is the plasma frequency of dust particles, ω_{piM} — plasma frequency of magnetospheric ions, ω_{Be} — electron gyrofrequency, $\mathbf{u}$ is the relative velocity of near-lunar dusty plasma and magnetospheric plasma motion, where the index $\parallel$ corresponds to the wave vector component parallel to the external magnetic field, $\cos\Theta = k_\parallel / |\mathbf{k}|$.

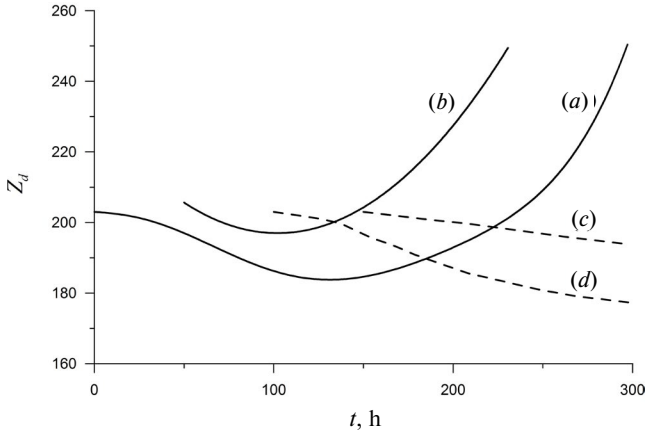

Fig. 3. Time dependencies of the charge number Z_d of dust particles with a radius of 0.1 μm in situations corresponding to different moments of dust particle detachment from the lunar surface: 0 (*a*), 50 (*b*), 100 (*c*), 150 (*d*) h.

In the situation corresponding to lower hybrid waves [44], at $\cos\Theta \ll 1$ and $|k_\parallel u_\parallel| \ll |\mathbf{k}\cdot\mathbf{u}|$ the dispersion equation (9) has the following unstable solution [20]:

$$\omega \approx \frac{\sqrt{\omega_{piM}^2+\omega_{pe(ph)}^2\cos^2\Theta}}{\sqrt{1+\omega_{pe(ph)}^2/\omega_{Be}^2}} + i\gamma^{Hydro} \equiv \equiv \omega_{LH}(\cos\Theta) + i\gamma^{Hydro}, \quad (10)$$

where γ^{Hydro} is the instability increment. The maximum increment values have the form

$$\gamma_{max}^{Hydro} = \frac{\sqrt{3}}{2^{4/3}}\omega_{LH}(\cos\Theta)\times \left(\frac{\omega_{pd}^2}{\omega_{piM}^2+\omega_{pe(ph)}^2\cos^2\Theta}\right)^{1/3} = \frac{\sqrt{3}}{2^{4/3}}\frac{\omega_{pd}}{\sqrt{1+\omega_{pe(ph)}^2/\omega_{Be}^2}}\times \left(\frac{\omega_{piM}^2+\omega_{pe(ph)}^2\cos^2\Theta}{\omega_{pd}^2}\right)^{1/6}. \quad (11)$$

The characteristic time of instability development

$$\tau = \left(\gamma_{max}^{Hydro}\right)^{-1}$$

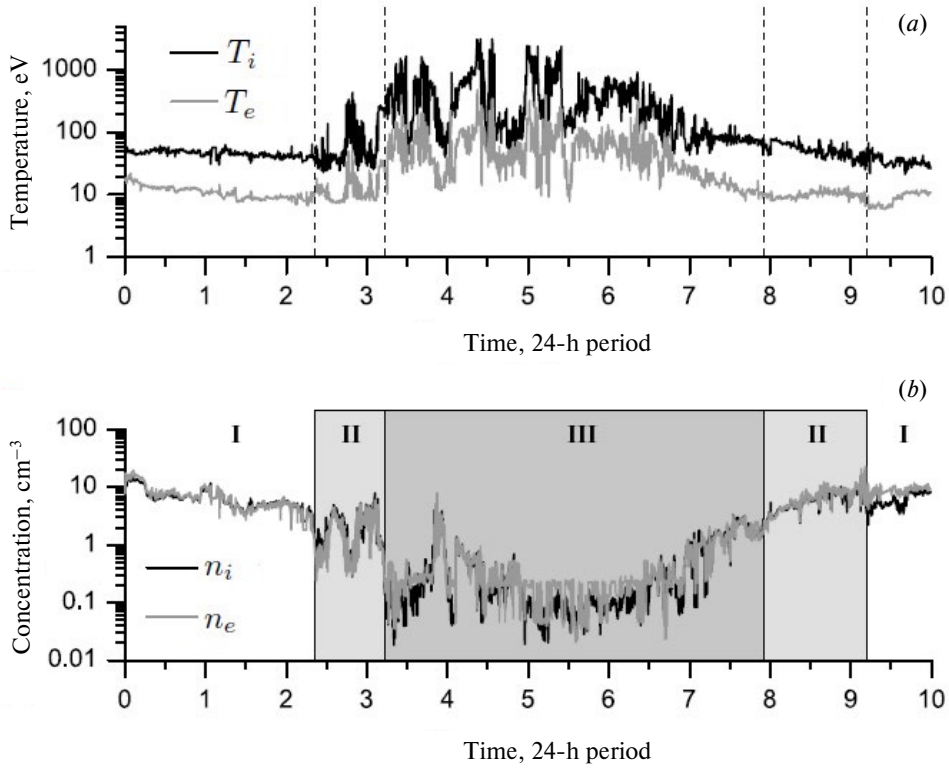

Fig. 4. Temperatures (a) and concentrations (b) of electrons and ions of solar wind and magnetosphere in lunar orbit, obtained from measurements by ARTEMIS P2 spacecraft during magnetospheric tail crossing from January 22 to 31, 2013 [46]. Roman numerals characterize regions of solar wind (I), magnetic transition and/or boundary layers of magnetosphere (II), inner part of magnetospheric tail (III), including plasma sheet. Boundaries between these regions are marked on panels (a) and (b) with vertical lines.

for photoelectron parameters ($n_{e(ph)} \sim 10^2$ cm^{-3}) from [45], corresponding to the quantum yield of lunar regolith given in [41], $|\mathbf{B}| \sim 10^{-4}$ Gs, $\cos\Theta \sim \omega_{piM} / \omega_{pe(ph)}$, $a \sim 100$ nm, $|Z_d| \sim 10$, $n_d \sim 10$ cm^{-3}, $n_{iM} \sim 10$ cm^{-3}, $m_d \sim 10^{-14}$ g is $\tau \approx 30$ s. The time (several days – see Fig. 4) during which the near-lunar dusty plasma interacts with Earth's magnetosphere significantly exceeds τ. Thus, one can expect the development of effective nonlinear processes associated with lower hybrid turbulence

The following scheme of plasma turbulence development is considered [20]. Magnetospheric plasma ions excite lower hybrid waves as a result of hydrodynamic instability development. Consequently (similar to the problem of anomalous plasma resistance [47]), there is an anomalous loss of ion momentum, which is transferred to waves. In the stationary saturation state, achieved when instability growth is limited by nonlinear processes, turbulent plasma heating occurs, the nature of which is determined by lower hybrid turbulence. Turbulent heating is uneven for ion and dust components.

To find the effective collision frequency ν_{eff}, which characterizes the anomalous loss of ion momentum, a quasi-linear interaction in the "magnetospheric ions + lower hybrid waves" system is considered, taking into account the fact that ions are unmagnetized, and also using the law of conservation of momentum and considering the friction force acting on ions due to their interaction with waves. As a result, we have

$$\nu_{eff} \approx \frac{1}{m_i n_{iM} u}\left|\int \gamma_{\mathbf{k}} W_{\mathbf{k}} \frac{\mathbf{k}}{\omega_{\mathbf{k}}} d\mathbf{k}\right| \sim \sim \frac{\omega_{pd}^{2/3}\omega_{LH}^{1/3}(\cos\Theta)}{\left(1+\omega_{pe(ph)}^2/\omega_{Be}^2\right)^{1/3}}\frac{v_{TiM}^2}{u^2}, \qquad (12)$$

where $\gamma_{\mathbf{k}}$ ($\omega_{\mathbf{k}}$) — imaginary (real) part of the frequency, $W_{\mathbf{k}}$ characterizes the wave spectrum in $\mathbf{k}$-space,

$$W = \int W_{\mathbf{k}} d\mathbf{k}$$

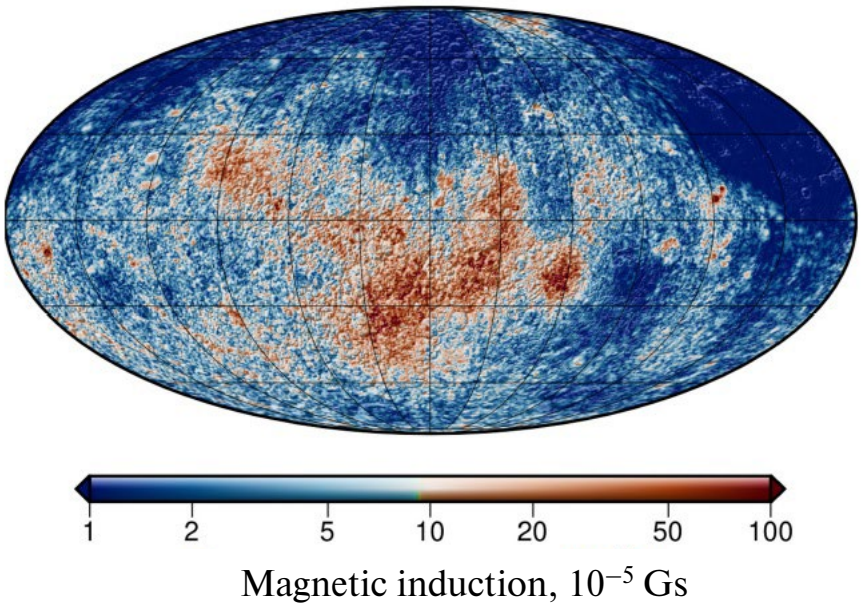

Fig. 5. Lunar magnetic field induction, constructed using a logarithmic color scale. The map is presented according to [52] in Mollweide equal-area projection, centered on the far side hemisphere of the Moon at 180° eastern longitude, with grid lines drawn every 30° in both latitude and longitude.

— energy density of lower hybrid waves, v_{TiM} — thermal velocity of magnetospheric ions. When deriving the final expression for ν_{eff} it was necessary to determine $W_{\mathbf{k}}$, for which nonlinear processes were considered. Since we are investigating the case when lower hybrid waves are excited as a result of hydrodynamic instability development, the analysis was conducted from the perspective of strong turbulence, when it becomes possible to obtain only order-of-magnitude estimates [48].

The value ν_{eff} allows, using relation $eE \sim \nu_{eff} m_i u$, to determine characteristic electric fields arising during the propagation of lower hybrid waves:

$$E \sim \frac{\omega_{pd}^{2/3}\omega_{LH}^{1/3}(\cos\Theta)}{\left(1+\omega_{pe(ph)}^2/\omega_{Be}^2\right)^{1/3}}\frac{T_{iM}}{eu}, \qquad (13)$$

where T_{iM} is the temperature of magnetospheric ions.

Calculations performed based on expression (13), for conditions corresponding to Earth's magnetosphere ($|\mathbf{B}| \sim 10^{-4}$ Gs, $\cos\Theta \sim \omega_{piM}/\omega_{pe(ph)}$, $a \sim 100$ nm, $u \sim 1$ km/s, $|Z_d| \sim 10$, $n_d \sim 10\,\text{cm}^{-3}$, $n_{iM} \sim 10\,\text{cm}^{-3}$, $m_d \sim 10^{-14}$ g, $T_{iM} \sim 100$ eV, $n_{e(ph)} \sim 10^2$ cm^{-3}), show that in the plasma-dust system near the Moon, as a result of lower-hybrid turbulence development, electric fields with amplitudes $E \sim 0.1$ B/m can be induced. This value is somewhat lower than the electric field value $E \sim 1$ B/m, excited near the Moon's surface due to its charging through interaction with solar radiation [14]. Nevertheless, electric fields excited by the development of lower-hybrid turbulence can affect the electric field pattern above the lunar surface, since the electric field arising from the interaction of solar radiation with the lunar surface decreases rather sharply with increasing altitude.

3. INFLUENCE OF MAGNETIC FIELDS IN MAGNETIC ANOMALY REGIONS

Currently, the Moon has no global magnetic field associated with eddy currents in its core. However, magnetic field measurements performed from orbit, as well as during Apollo missions 12, 14, 15 and 16, show that some areas of the lunar crust are strongly magnetized [3, 49, 50]. Additionally, some lunar samples collected from the Moon's surface are magnetized [51, 52]. All this indicates the existence of strong magnetic anomalies on the Moon. Fig. 5 presents a map characterizing the magnetic field induction in lunar magnetic anomaly zones.

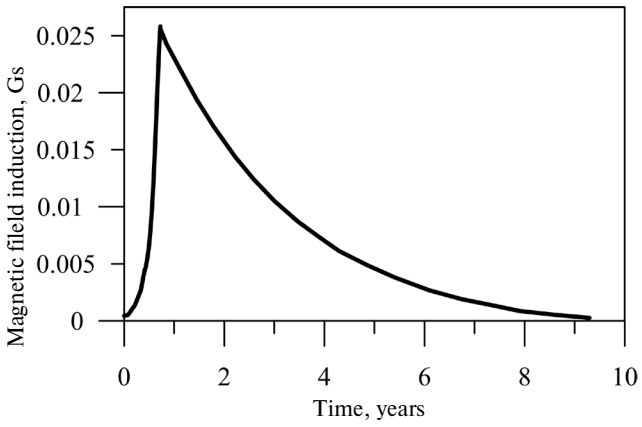

Fig. 6. Calculated time dependence of magnetic field induction near the lunar surface [5], formed as a result of launching the lunar dynamo due to the impact of a cosmic body on the lunar surface

As noted in the Introduction, magnetic fields in magnetic anomaly regions can exceed the Earth's magnetosphere magnetic fields existing in the lunar orbit by one to two orders of magnitude. Moreover, based on the analysis of possible mechanisms for the origin of lunar magnetic anomalies, it is possible to estimate the maximum possible magnetic fields near the lunar surface. Fig. 6 shows the calculated time dependence of the magnetic field induction near the lunar surface, formed within the mechanism associated with the impact of a cosmic body on the lunar surface [5]. This creates large-scale fluid flows in the lunar core, excited by tidal distortion of the core-mantle boundary, which activates the lunar dynamo mechanism. The surface magnetic field strength predicted within this mechanism is about 10^{-2} Gs, which is consistent with paleomagnetic measurements [51], and the duration of these fields is sufficient to explain the central magnetic anomalies associated with several large impact basins on the Moon.

Below, we examine the influence of magnetic fields in magnetic anomaly regions on the properties of the plasma-dust system near the Moon, and discuss the properties and manifestations of minimagnetspheres.

3.1. The influence of lunar magnetic anomalies on the plasma-dust system

For analyzing the influence of magnetic fields in magnetic anomaly regions on the evolution of the plasma-dust system, it is important that both the magnetic field and dusty plasma in the considered situation are "tied" to the lunar surface. The velocity entering the magnetic part of the Lorentz force in this case has the order of magnitude u_d, shown in Fig. 2, i.e. ~ 10 m/s unlike the situation of the Earth's magnetosphere magnetic field, where the dust particle velocity relative to the magnetic field is greater than or about 1 km/s. Thus, the magnetic part of the Lorentz force acting on a dust particle for magnetic anomaly fields is either less than or comparable to the similar force calculated for the Earth's magnetosphere tail magnetic fields in lunar orbit. At the same time, magnetic fields in magnetic anomaly regions can lead to changes in dust particle trajectories, deflecting them from those shown in Fig. 2. Since the characteristic sizes of magnetic anomaly regions are about 10–100 km (see, for example, [5]), the general tendency of dust particle movement shown in Fig. 2 remains. That is, due to the fact that magnetic anomaly regions are significantly localized, their influence on the transport of charged dust particles above the Moon does not lead to new qualitative effects.

However, lunar magnetic anomalies may significantly influence dusty plasma parameters above certain areas of the Earth's satellite territory. Indeed, it is possible to identify the following ranges of magnetic field values near the lunar surface.

1. $|\mathbf{B}| \ll 10^{-5}$ Gs. In this case, solar wind electrons and protons reach the lunar surface, and the presence of a magnetic field essentially does not affect the properties of the plasma-dust system.

2. 10^{-5} Gs $\ll |\mathbf{B}| \ll 5 \cdot 10^{-3}$ Gs. In this case, solar wind electrons do not reach the lunar surface, while most solar wind protons do reach it. This magnetic field range corresponds to most lunar magnetic anomaly zones.

3. $|\mathbf{B}| \gg 5 \cdot 10^{-3}$ Gs. In this case, both solar wind electrons and ions cannot reach the lunar surface.

Accordingly, plasma-dust system parameters above the lunar surface can be calculated for each of these magnetic field ranges.

As noted above, for the Moon, it can be assumed that there is a balance between electrostatic and gravitational forces for a dust particle, i.e., the particle levitates at a certain height. Then, to describe the behavior of levitating dust particles in the case of $|\mathbf{B}| \ll 10^{-5}$ Gs and determine their height distributions, instead of the system of differential

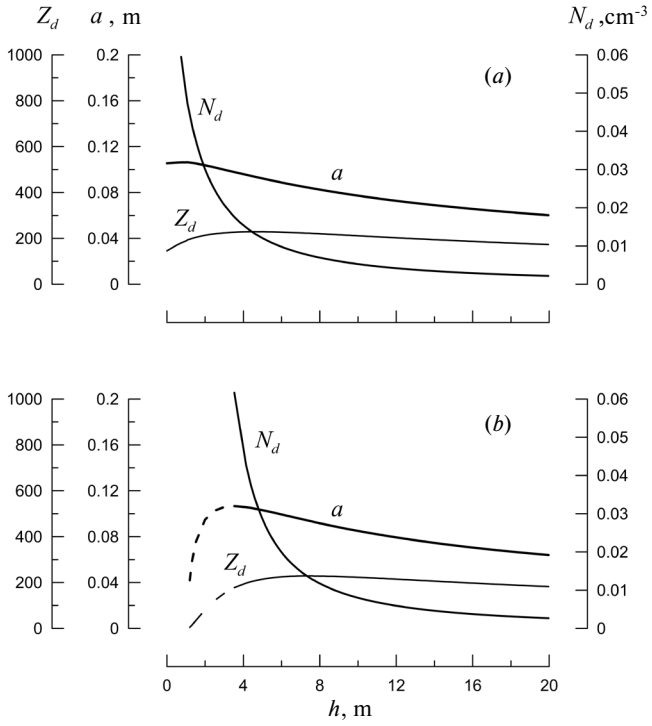

Fig. 7. Dependencies of radius a, charge number Z_d of dust particles and their concentrations N_d on height h in the equilibrium vertical position above the lunar surface for values $\theta = 87^\circ$ (a), 0° (b) in the case of $|\mathbf{B}| \ll 10^{-5}$ Gs. Solid lines correspond to stable equilibrium, dashed lines – to unstable equilibrium can be considered levitating.

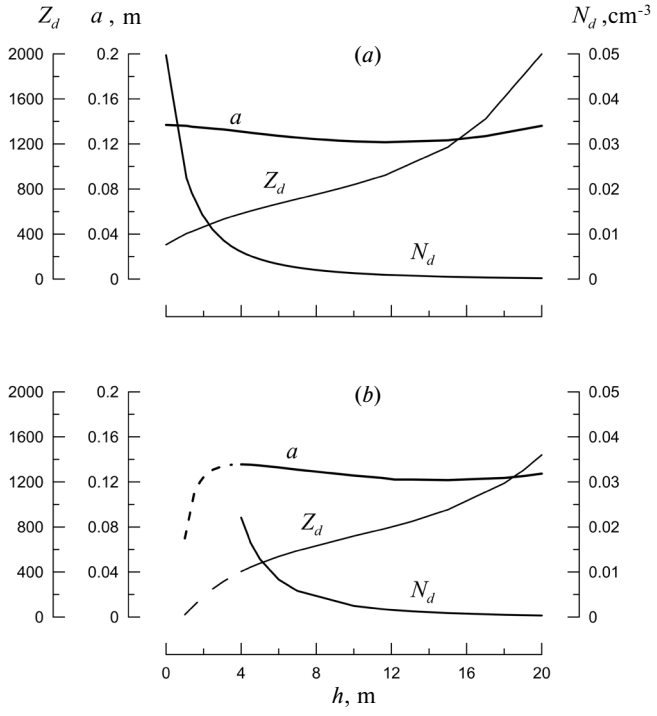

Fig. 8. Dependencies of radius a, charge number Z_d of dust particles and their concentrations N_d on height h in equilibrium vertical position above the lunar surface for values θ=87° (a), 0° (b) in case 10^{-5} Gs $\ll |\mathbf{B}| \ll 5 \cdot 10^{-3}$ Gs. Solid lines correspond to stable equilibrium, dashed lines – to unstable equilibrium can be considered levitating.

equations (1) and (2), the following system of algebraic equations should be solved:

$$q_d \mathbf{E} + m_d g_0 = 0, \tag{14}$$

$$I_e(q_d) + I_i(q_d) - I_{ph}(q_d) + I_{e,ph}(q_d) = 0. \tag{15}$$

Fig. 7 shows the dependencies of size a, charge number Z_d of dust particles and their concentrations N_d in the equilibrium vertical position, characterized by height h, on this height for different values of angle θ. The sizes of dust particles (from 0.068 to 0.105 μm), shown in Fig. 7 correspond to the situation when dust particles Fig. 7 highlights situations of unstable and stable equilibria. Any small displacement (in the vertical direction) of a dust particle from the state of unstable equilibrium leads to the particle falling, which is due to the dominance of gravitational attraction force over electrostatic force after the particle is moved from the unstable equilibrium state. If a dust particle is displaced from a stable equilibrium position, it will tend to return to this position.

The case of 10^{-5} Gs $\ll |\mathbf{B}| \ll 5 \cdot 10^{-3}$ Gs the following system of algebraic equations is valid:

$$q_d \mathbf{E} + m_d \mathbf{g}_0 = 0, \tag{16}$$

$$I_i(q_d) - I_{ph}(q_d) + I_{e,ph}(q_d) = 0. \tag{17}$$

Solving it, we find the dependencies of size and charge number of dust particles, as well as their concentrations in the equilibrium vertical position on height for different values of angle θ. The corresponding dependencies are shown in Fig. 8.

Case $|\mathbf{B}| \gg 5 \cdot 10^{-3}$ Gs is described using the following system of algebraic equations:

$$q_d \mathbf{E} + m_d \mathbf{g}_0 = 0, \tag{18}$$

$$-I_{ph}(q_d) + I_{e,ph}(q_d) = 0. \tag{19}$$

Its solutions are shown in Fig. 9.

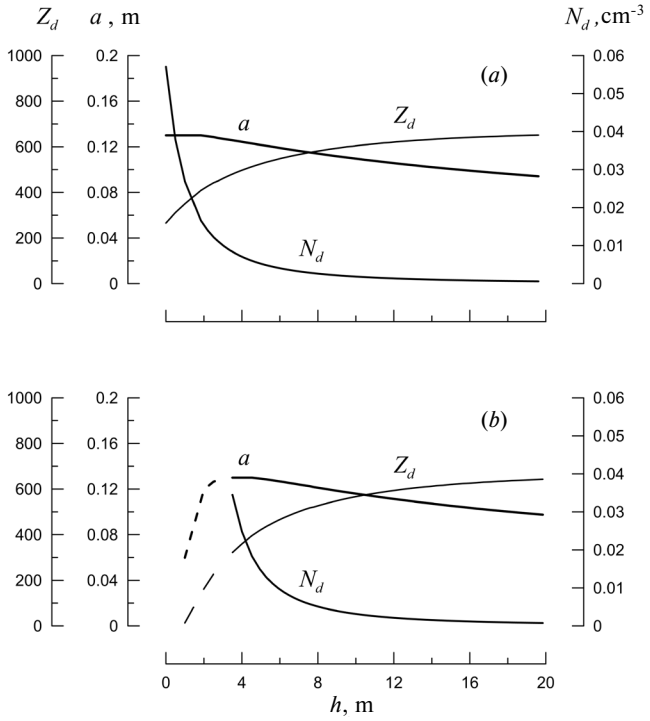

Fig. 9. Dependencies of radius a, charge number Z_d of dust particles and their concentrations N_d on height h in the equilibrium vertical position above the lunar surface for values $\theta = 87°$ (*a*), 0° (*b*) in the case of $|\mathbf{B}| \gg 5 \cdot 10^{-3}$ Gs. Solid lines correspond to stable equilibrium, dashed lines – to unstable equilibrium can be considered levitating.

Comparison of results presented in Fig. 7–9, shows that in case 10^{-5} Gs $\ll |\mathbf{B}| \ll 5 \cdot 10^{-3}$ Gs dust particle concentrations are minimal (compared to other cases), although larger particles rise above the lunar surface. As already noted, this case corresponds to the majority of lunar magnetic anomaly zones. Thus, in magnetic anomaly zones, dusty plasma is "suppressed" compared to the situation outside these zones.

3.2. Mini-magnetospheres

"Lunar swirls" are optically distinguishable, sufficiently bright (often interpreted as white) elements of the lunar surface, differing in their structural details from craters and impact ejecta (see fig. 10). They are found in several locations on the lunar surface [53]. It has been established that their shape is not related to topographic features and apparently overlays both mountainous terrain and plateaus [54–56]. Although not all magnetic anomaly zones have identifiable "lunar swirls," no "lunar swirls" have been discovered that do not coincide with lunar magnetic anomaly zones of similar size [56, 57].

Proton bombardment from the solar wind eventually leads to reddening (darkening) of the lunar regolith [59]. A decrease in proton flux over an extended period results in a "lighter" color of the lunar surface, while additional enhancement of proton flux leads to an even "darker" appearance. The interaction between these two factors results in the formation of "white stripes" alternating with narrow "dark bands" [56, 57] in "lunar swirls" and their surroundings.

These spectroscopic features allowed interpreting "lunar swirls" as a diagnostic observation directly related to the interaction between solar wind and mini-magnetospheres above lunar magnetic anomaly zones [33]. Such interaction leads to the deflection of solar wind protons from the "lunar swirl" zone [57]. As a result, protons end up on the lunar surface outside the "lunar swirl" zone. Additional concentration of protons in narrow "dark bands" [56] significantly enhances the spectral darkening effects caused by space weathering compared to the normal lunar surface.

Mini-magnetospheres in lunar magnetic anomaly regions possess features characteristic of regular planetary magnetospheres, namely a collisionless bow shock. It turns out that electric fields associated with the collisionless shock wave bounding mini-magnetospheres lead to the deflection of incoming solar wind protons from their initial propagation direction [34]. These ions, upon impacting the lunar surface, cause changes in the appearance of lunar soil albedo [57]. Thus, the shape of swirl patterns in "lunar swirls" and their surroundings is determined by the form of the collisionless shock wave.

Such collisionless shock waves have a characteristic structure where ions are reflected (or deflected) from a rather narrow layer, on the order of electron skin depth c / ω_{pe}, by an electrostatic field arising from the interaction of magnetized electrons and unmagnetized ions, which corresponds to the range of 10^{-5} Gs $\ll |\mathbf{B}| \ll 5 \cdot 10^{-3}$ Gs. Note that since not all magnetic anomaly zones have identifiable "lunar swirls," the effect of ion reflection or deflection from the collisionless bow shock does not occur for all magnetic anomaly zones. In this case, the description given in Section 3.1. is valid. Otherwise, the effect of ion reflection or deflection should be taken into account.

Fig. 10. On the left side of the image is an example of "lunar swirls" in the lunar magnetic anomaly region of Reiner Gamma (7.4° north latitude, 300.9° east longitude). The Reiner Gamma region is named after the impact crater "Reiner," shown for comparison on the right. Information taken from the "Scientific Russia" portal [58]

Since analytical study of mini-magnetospheres is difficult, at least due to their complex geometry, laboratory experiments are conducted to study mini-magnetospheres and account for the effects of ion reflection or deflection from the bow shock using, for example, a plasma wind tunnel [33, 34]. It turns out that mini-magnetospheres obtained in laboratory conditions have characteristics similar to lunar mini-magnetospheres. Quantitative agreement of observations both in space and in the laboratory is also achieved.

Numerical studies of mini-magnetospheres are also being conducted using the OSIRIS particle-in-cell method [33]. This code contains few physical approximations and is suitable for studying complex systems with many degrees of freedom, such as lunar mini-magnetospheres. MHD codes cannot be used because the size of the mini-magnetosphere structure is much smaller than what the MHD code allows. Within the calculations using the OSIRIS code, it is possible, in particular, to identify various types of plasma waves observed in magnetic anomaly zones, such as whistlers and lower hybrid waves [60–62]. Three-dimensional calculations [33] showed, in particular, how electrostatic fields of various orientations are formed in the bow shock, resulting in the formation of a protective "dome" that scatters incoming protons, thereby reducing the flux of protons reaching the lunar surface. These calculations also illustrated the possibility of forming propagation directions of scattered protons where their concentration increases, and, accordingly, when these protons interact with the lunar surface, they create "dark lanes" in the areas of "lunar swirls". Thus, the numerical modeling data confirm the hypothesis that the observed spectral effects characterizing "lunar swirls" are due to the differentiation of solar wind proton propagation directions during their interaction with mini-magnetospheres. A consequence of this consideration is, for example, the fact that for different "lunar swirls", the width of the "dark lanes" should be approximately the same.

The electrostatic potential φ, responsible for slowing down and deflecting protons from their initial propagation direction, equals [34]

$$\varphi = -\frac{B^2}{8\pi ne}. \tag{20}$$

With the particle concentration in the solar wind $n \approx 5\,\text{cm}^{-3}$ and magnetic field in the lunar magnetic anomaly zone $B \approx 3 \cdot 10^{-4}$ Gs, corresponding to Lunar Prospector measurement data [63], the theoretical value φ equals ~ 450 V [34], which is in accordance with observational data ~ 400 V [64].

Proton flows formed as a result of reflection (or deflection) from the collisionless bow shock lead to the development of modified two-stream instability and generation of lower hybrid waves [65] at frequencies close to $\sqrt{\omega_{Be}\omega_{Bi}}$, where ω_{Bi} is the ion gyrofrequency. Comparison of this frequency with frequencies of 1–10 Hz, at which intense electrostatic oscillations were observed by the Nozomi spacecraft [62], indicates good agreement between theory and experiment [33].

Furthermore [33], lower hybrid waves generated by modified two-stream instability are responsible for electron acceleration, which was also observed in satellite measurements. It should be noted that lower hybrid waves are highly effective as an electron acceleration mechanism. Taking into account this acceleration mechanism, it becomes possible to obtain the thickness of the collisionless shock wave layer from which ions are reflected (or deflected) [34]. It turns out that the thickness of this layer is on the order of the electron skin depth, ranging from 1 to 2 km, rather than hundreds of kilometers corresponding to the ion skin depth [66].

Thus, there are substantial grounds to consider mini-magnetospheres as an important factor associated with lunar magnetic anomaly zones and responsible for a number of lunar optical observations, such as "lunar swirls", as well as satellite measurements of plasma effects, for example, lower hybrid turbulence. Apparently, mini-magnetospheres do not always significantly affect the propagation of solar wind ions. Otherwise, effects such as "lunar swirls" would be observed in the vicinity of all lunar magnetic anomaly zones.

4. CONCLUSION

Thus, due to the action of magnetic fields in Earth's magnetospheric tail, the transport of charged dust particles over the lunar surface is possible over large distances. Consequently, dusty plasma above the sunlit lunar surface can exist for the entire range of lunar latitudes. The magnetic component of the Lorentz force acting on a dust particle for magnetic anomaly fields is either smaller than or comparable to the similar force calculated for the Earth's magnetospheric tail fields at lunar orbit. However, due to the significant localization of magnetic anomaly regions, their influence on the transport of charged dust particles over the Moon is insignificant. Nevertheless, in magnetic anomaly zones, dusty plasma is "suppressed" compared to the situation outside these zones. An important object of study is mini-magnetospheres associated with lunar magnetic anomaly zones and responsible for a number of optical and satellite observations, such as "lunar swirls", lower hybrid turbulence, etc.

REFERENCES

1. E. W. Hones, Jr., Aust. J. Phys. 38, 981 (1985).
2. Y. Harada, Interactions of Earth's Magnetotail Plasma with the Surface, Plasma, and Magnetic Anomalies of the Moon, Springer, Japan (2015).
3. P. Dyal, C. W. Parkin, and W.D.Daily, Rev. Geophys. 12, 568 (1974).
4. P. J. Coleman, Jr., G. Schubert, C.T. Russell, and L. R. Sharp, Moon 4, 419 (1972).
5. M. Le Bars, M. A. Wieczorek, Ö. Karatekin, D. Cébron, and M. Laneuville, Nature 479, 215 (2011).
6. M. A. Wieczorek, B.P.Weiss, and S.T.Stewart, Science 335, 1212 (2012).
7. M. A. Wieczorek, J. Geophys. Res.: Planets 123, 291 (2018).
8. E. F. Lyon, H.S. Bridge, and J. H. Binsack, J. Geophys. Res. 72, 6113 (1967).
9. L. Hood and N. Artemieva, Icarus 193, 485 (2008).
10. M. A. Wieczorek and M. Lefeuvre, Icarus 200, 358 (2009).
11. T. J. Stubbs, R. R. Vondrak, and W. M. Farrell, Adv. Space Res. 37, 59 (2006).
12. S. I. Popel, L. M. Zelenyi, A. P. Golub', and A. Yu. Dubinskii, Planet. Space Sci. 156, 71 (2018).
13. J. E. Colwell, S. Batiste, M. Horányi, S. Robertson, and S. Sture, Rev. Geophys. 45, RG2006 (2007).
14. S. I. Popel, S. I. Kopnin, A. P. Golub, G. G. Dolnikov, A. V. Zakharov, L. M. Zelenyi, Yu. N. Izvekova, Solar System Research 47, 419 (2013)
15. S.I.Popel, G.E. Morfill, P.K. Shukla, and H. Thomas, J. Plasma Phys. 79, 1071 (2013).
16. S. I. Popel, L. M. Zelenyi, and B. Atamaniuk, Phys. Plasmas 22, 123701 (2015).
17. T. I. Morozova, S. I. Kopnin, S. I. Popel, Plasma Physics Physi. Plasmas 41, 867 (2015).
18. S. I. Popel, T. I. Morozova, Plasma Physics 43, 474 (2017).
19. Yu. N. Izvekova, T. I. Morozova, and S. I. Popel, IEEE Trans. Plasma Sci. 46, 731 (2018).
20. S.I.Popel, A. I. Kassem, Yu.N. Izvekova, and L. M. Zelenyi, Phys. Lett. A 384, 126627 (2020).

21. S. I. Popel, A. P. Golub, E. A. Lisin, Yu. N. Izvekova, B. Atamaniuk, G. G. Dolnikov, A. V. Zakharov, L. M. Zelenyi, JETP Letters 103, 641 (2016).

22. S. I. Popel, A. P. Golub, L. M. Zelenyi, M. Horanyi, JETP Letters 105, 594 (2017).

23. A. P. Golub, S. I. Popel, Solar System Research 55, 393 (2021).

24. E. Walbridge, J. Geophys. Res. 78, 3668 (1973).

25. M. Horányi, Z. Sternovsky, M. Lankton, C. Dumont, S. Gagnard, D. Gathright, E. Grün, D. Hansen, D. James, S. Kempf, B. Lamprecht, R. Srama, J. R. Szalay, and G. Wright, Space Sci. Rev. 185, 93 (2014).

26. D. Li, Y. Wang, H. Zhang, X. Wang, Y. Wang, Z. Sun, J. Zhuang, C. Li, L. Chen, H. Zhang, X. Zou, C. Zong, H. Lin, J. Ma, X. Li, X. Cui, R. Yao, X. Wang, X. Gao, Sh. Yang, X. Wang, and B.Zhang, Geophys. Res. Lett. 47, e2020GL089433 (2020).

27. L. M. Zelenyi, S. I. Popel, A. V. Zakharov, Plasma Physics Reports 46, 441 (2020).

28. A. V. Zakharov, L. M. Zelenyi, S. I. Popel, Solar System Research 54, 483 (2020) Phys. Plasmas.

29. R. Bamford, K. J. Gibson, A. J. Thornton, J. Bradford, R. Bingham, L. Gargate, L. O. Silva, R. A. Fonseca, M. Hapgood, C. Norberg, T. Todd, and R. Stamper, Plasma Phys. Control. Fusion 50, 124025 (2008).

30. L. Gargaté, R. Bingham, R. A. Fonseca, R. Bamford, A. Thornton, K. Gibson, J. Bradford, and L. O. Silva, Plasma Phys. Control. Fusion 50, 074017 (2008).

31. A. R. Poppe, J.S.Halekas, G.T.Delory, and W. M. Farrell, J. Geophys. Res. 117, A09105 (2012).

32. J. Deca, A. Divin, G.Lapenta, B. Lembège, S. Markidis, and M. Horányi, Phys. Rev. Lett. 112, 151102 (2014).

33. R. A. Bamford, E. P. Alves, F. Cruz, B. J. Kellett, R. A. Fonseca, L. O. Silva, R. M. G. M. Trines, J. S. Halekas, G. Kramer, E. Harnett, R. A. Cairns, and R. Bingham, Astrophys. J. 830, 146 (2016).

34. R. A. Bamford, B. Kellett, W. J. Bradford, C. Norberg, A. Thornton, K. J. Gibson, I. A. Crawford, L. Silva, L. Gargaté, and R. Bingham, Phys. Rev. Lett. 109, 081101 (2012).

35. L. L. Hood and G. Schubert, Science 208, 49 (1980).

36. S.I. Popel, A.P. Golub', A.I.Kassem, and L. M. Zelenyi, Phys. Plasmas 29, 013701 (2022).

37. R. J. L. Grard and J. K. E. Tunaley, J. Geophys. Res. 76, 2498 (1971).

38. E. K. Kolesnikov, A. S. Manuylov, Astron. Zh. J. Solar System Research 59, 996 (1982).

39. E. K. Kolesnikov, A. B. Yakovlev, Astron. Vestn. Solar System Research 31, 70 (1997).

40. S. I. Popel, A. P. Golub, JETP Letters 115, 629 (2022).

41. R.F. Willis, M. Anderegg, B. Feuerbacher, and B. Fitton, in Photon and Particle Interactions with Surfaces in Space, ed. by R. J. L. Grard and D. Reidel, Dordrecht (1973), p. 389.

42. Y. Asano, I. Shinohara, A. Retinò, P. W. Daly, E. A. Kronberg, T. Takada, R. Nakamura, Y. V. Khotyaintsev, A. Vaivads, T. Nagai, W. Baumjohann, A.N.Fazakerley, C. J. Owen, Y. Miyashita, E. A. Lucek, and H. Rème, J. Geophys. Res. 115, 05215 (2010).

43. O. Buneman, Phys. Rev. 115, 603 (1959).

44. S. I. Popel, S. V. Vladimirov, and V.N.Tsytovich, Phys. Rep. 259, 327 (1995).

45. S. I. Popel, A. P. Golub, Yu. N. Izvekova, V. V. Afonin, G.G.Dolnikov, A. V. Zakharov, L.M.Zelenyi, E. A. Lisin, O.F.Petrov, JETP Letters 99, 131 (2014).

46. J. Vaverka, I. Richterová, J. Pavlů, J. Šafránková, and Z. Němeček, Astrophys. J. 825, 133 (2016).

47. A. A. Galeev, R.Z.Sagdeev, Problems of Plasma Theory, Issue 7, ed. by M.A. Leontovich, Atomizdat, Moscow (1973), p. 3.

48. S. V. Vladimirov, V.N. Tsytovich, S.I. Popel, and F.Kh.Khakimov, Modulational Interactions in Plasmas, Kluwer Acad. Publ., Dordrecht-Boston-London (1995).

49. L. L. Hood, A.Zakharian, J. Halekas, D. L. Mitchell, R. P. Lin, M. H. Acu na, and A. B. Binder, J. Geophys. Res. 106, 27825 (2001).

50. H. Tsunakawa, H. Shibuya, F. Takahashi, H. Shimizu, M. Matsushima, A. Matsuoka, S. Nakazawa, H. Otake, and Y.Iijima, Space Sci. Rev. 154, 219 (2010).

51. I. Garrick-Bethell, B. P. Weiss, D. L. Shuster, and J. Buz, Science 323, 356 (2009).

52. S. Gong and M.A.Wieczorek, J. Geophys. Res.: Planets 125, e2019JE006274 (2020).

53. F. El-Baz, Apollo 16: Preliminary Science Report, NASA Spec. Publ. SP 315, 29 (1972).

54. J. F. Bell and B. R. Hawke, Publ. Astron. Soc. Pacific 99, 862 (1987).

55. P. C. Pinet, V. V. Shevchenko, S. D. Chevrel, Y. Daydou, and C. Rosemberg, J. Geophys. Res.: Planets 105, 9457 (2000).

56. D. Blewett, B. Hawke, N. Richmond, and C. Hughes, Geophys. Res. Lett. 34, L24206 (2007).

57. G. Y.Kramer, S. Besse, D. Dhingra, J. Nettles, R. Klima, I. Garrick-Bethell, R. N. Clark, J.-P. Combe, J. W. Head III, L. A. Taylor, C. M. Pieters, B. Boardman, and T.B. McCord, J. Geophys. Res. 116, E00G18 (2011).

58. https://scientificrussia.ru/articles/obnaruzeny-lunnye-kamni-s-unikalnoj-pylu

59. C. Pieters, E. Fischer, O. Rode, and A. Basu, J. Geophys. Res.: Planets 98, 20817 (1993).

60. J. Halekas, D. Brain, D. Mitchell, and R. Lin, Geophys. Res. Lett. 33, 22 (2006).

61. T. Nakagawa, F. Takahashi, H. Tsunakawa, H. Shibuya, H. Shimizu, and M. Matsushima, Earth, Planets and Space 63, 37 (2011).

62. Y. Futaana, S. Machida, Y. Saito, A. Matsuoka, and H. Hayakawa, J. Geophys. Res. 108, 1025 (2003).

63. R.P.Lin, D.L.Mitchell, D. W. Curtis, K. A. Anderson, C. W. Carlson, J. McFadden, M. H. Acu na, L. L. Hood, and A.Binder, Science 281, 1480 (1998).

64. Y. Futaana, S. Barabash, M. Wieser, M. Holmström, A. Bhardwaj, M. B. Dhanya, R. Sridharan, P. Wurz, A. Schaufelberger, and K. Asamura, J. Geophys. Res.: Space Phys. 115, A10248 (2010).

65. R. Bingham, R. Bamford, B. J. Kellett, and V. D. Shapiro, J. Plasma Phys. 76, 915 (2010).

66. A. D. R. Phelps, Planet. Space Sci. 21, 1497 (1973).